Synthesis of Mesoporous Carbons Using Ordered and Disordered Mesoporous Silica Templates and Polyacrylonitrile as Carbon Precursor

Michal Kruk,*,† Bruno Dufour,† Ewa B. Celer,‡ Tomasz Kowalewski,*,† Mietek Jaroniec,‡ and Krzysztof Matyjaszewski*,†

Department of Chemistry, Carnegie Mellon University, 4400 Fifth Avenue, Pittsburgh, Pennsylvania 15213, and Department of Chemistry, Kent State University, Kent, Ohio 44242

Received: September 28, 2004; In Final Form: February 2, 2005

Mesoporous carbons were synthesized from polyacrylonitrile (PAN) using ordered and disordered mesoporous silica templates and were characterized using transmission electron microscopy (TEM), powder X-ray diffraction, nitrogen adsorption, and thermogravimetry. The pores of the silica templates were infiltrated with carbon precursor (PAN) via polymerization of acrylonitrile from initiation sites chemically bonded to the silica surface. This polymerization method is expected to allow for a uniform filling of the template with PAN and to minimize the introduction of nontemplated PAN, thus mitigating the formation of nontemplated carbon. PAN was stabilized by heating to 573 K under air and carbonized under N_2 at 1073 K. The resulting carbons exhibited high total pore volumes (1.5−1.8 $cm^3\ g^{-1}$), with a primary contribution of the mesopore volume and with relatively low microporosity. The carbons synthesized using mesoporous templates with a 2-dimensional hexagonal structure (SBA-15 silica) and a face-centered cubic structure (FDU-1 silica) exhibited narrow pore size distributions (PSDs), whereas the carbon synthesized using disordered silica gel template had broader PSD. TEM showed that the SBA-15-templated carbon was composed of arrays of long, straight, or curved nanorods aligned in 2-D hexagonal arrays. The carbon replica of FDU-1 silica appeared to be composed of ordered arrays of spheres. XRD provided evidence of some degree of ordering of graphene sheets in the carbon frameworks. Elemental analysis showed that the carbons contain an appreciable amount of nitrogen. The use of our novel infiltration method and PAN as a carbon precursor allowed us to obtain ordered mesoporous carbons (OMCs) with (i) very high mesopore volume, (ii) low microporosity, (iii) low secondary mesoporosity, (iv) large pore diameter (8−12 nm), and (v) semi-graphitic framework, which represent a desirable combination of features that has not been realized before for OMCs.

Introduction

Mesoporous carbons, that is, carbons with pores of diameter in the range from 2 to 50 nm, have recently attracted much attention,[1−14] which was fostered by prospects of their applications as adsorbents for large, hydrophobic molecules and biomolecules;[15−17] catalyst supports;[18] components of electrochemical double-layer capacitors,[2,19−26] fuel cells[3,27,28] and Li-ion batteries;[29,30] chromatographic packings;[31] and templates for the synthesis of inorganic nanostructures.[32−37] There are numerous ways to synthesize mesoporous carbons, including (i) physical activation of carbon to high burnoff degree,[38] (ii) combination of physical and chemical activation,[39] (iii) carbonization of polymer blends with one unstable component,[40] (iv) carbonization of polymer aerogels[41] or cryogels,[42] (v) templating with porous silicas[43] or silica particles,[4,7] either preformed or formed in situ during the polymerization of carbon precursor,[6] and (vi) a variety of methods to produce multiwall carbon nanotubes.[44] The templating with porous silicas is particularly attractive; in fact, it is a method currently used to prepare mesoporous carbons for applications in liquid chromatography.[43,45] In 1999, the research on the synthesis of mesoporous carbons using silica templates gained new momentum, when two research groups reported the successful synthesis of ordered mesoporous carbons (OMCs)[1,2] using ordered mesoporous silicas[46−48] as templates. This novel approach has been actively pursued over the last four years, leading to the synthesis of OMCs with a variety of structures, including (i) a structure consisting of two separate, but intertwined, systems of rods with three-way intersections, which has an $I4_1/a$ symmetry,[49] (ii) 2-D hexagonal (*p*6*mm*) arrays of rods or tubes,[3,50] (iii) cubic *Ia*3*d* structure (similar to that described in (i) but with higher symmetry),[19,49] (iv) cubic *Pm*3*n* structure,[9,51] (v) cubic *Im*3*m* (body-centered) structure,[52] and (vi) cubic *Fm*3*m* (face-centered) structure.[52] Disordered carbons with very large, spherical mesopores were also obtained.[53] This progress in the synthesis of ordered mesoporous carbons was paralleled by significant progress in the synthesis of other kinds of mesoporous carbons, using silica particles[4,5,7] (including hard-core/mesoporous-shell silica particles),[54] disordered silicas[8,14] and in situ formed silica structures[6] as imprinting media,[7] templates,[8,14] and porogens[4,5] or in situ generated porogens.[6]

One of the focal points in the current effort on the synthesis of OMCs is the identification of carbon precursors, which would be the most beneficial from the point of view of fabrication and prospective applications of these carbons. Sucrose is perhaps the most commonly used carbon precursor,[1] but polymers

* Corresponding authors. M. Kruk: tel. (412) 268-9175, fax (412) 268-1061, e-mail: mkruk@andrew.cmu.edu; T. Kowalewski: tel. (412) 268-5927, fax (412) 268-1061, e-mail: tomek@andrew.cmu.edu; K. Matyjaszewski: tel. (412) 268-3209, fax (412) 268-6897, e-mail: km3b@andrew.cmu.edu.

† Carnegie Mellon University.

‡ Kent State University.

10.1021/jp045594x CCC: $30.25
Published on Web 04/15/2005

SCHEME 1: Synthesis of Ordered Mesoporous Carbon Using Silica Template and Carbon Precursor Formed via Surface-Initiated Controlled Radical Polymerization

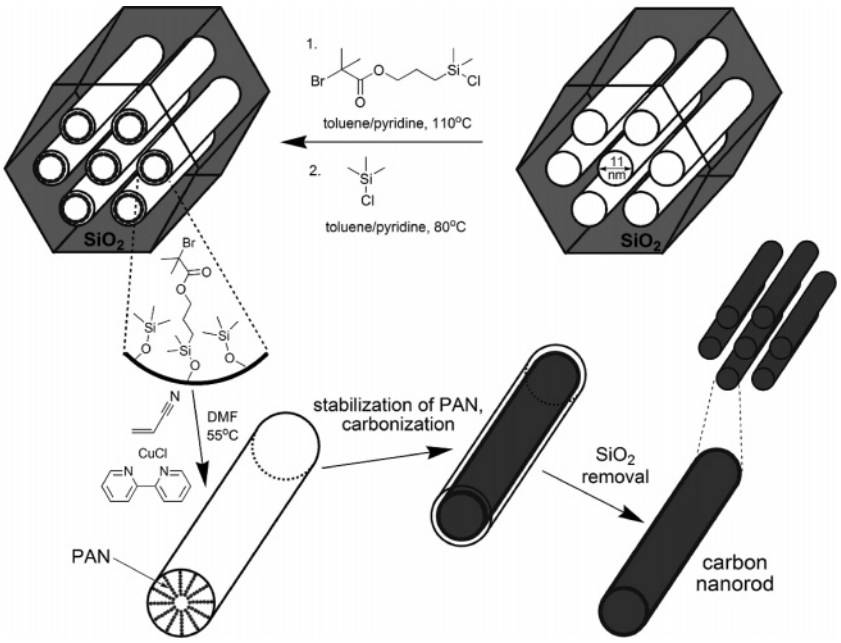

formed in situ in the pores of the template are also frequently employed. These polymers include (i) phenolic resin formed from phenol and formaldehyde,[1,2] (ii) poly(furfuryl alcohol),[1,3,55−57] (iii) poly(divinylbenzene),[58−60] (iv) polyacrylonitrile (PAN),[61,62] and poly(vinyl chloride).[63] The polymerizations of furfuryl alcohol and phenol/formaldehyde were initiated by acidic sites (such as aluminum heteroatoms,[1,2] surface-bonded sulfonic acid groups,[57] or *p*-toluenesulfonic acid[64]), which needed to be introduced on the surface of the silica template. Aromatic and polyaromatic hydrocarbons, including acenaphthene,[65] benzene, naphthalene, antracene, and pyrene,[66] constitute another important group of carbon precursors. Petroleum pitch[67,68] and mesophase pitch,[69−71] which are composed primarily of polyaromatic hydrocarbons, are also very promising carbon precursors for the synthesis of ordered mesoporous carbons. In addition, one can form carbon from propylene,[72] acetylene,[49] ethylene,[73] styrene,[74,75] furfuryl alcohol,[55] and acetonitrile[75,76] using chemical vapor deposition (CVD) techniques. Alkylammonium surfactants and block copolymers, which serve as supramolecular templates for the synthesis of ordered mesoporous silica templates, can also serve as auxiliary carbon precursors (in the case of alkylammonium surfactants, which increased carbon yield, when poly(divinylbenzene) was used as the main carbon source),[59] or even as a sole carbon source[77] (in the case of poly(ethylene oxide)−poly(propylene oxide)−poly(ethylene oxide) triblock copolymers). The use of the polymer template as a carbon source follows an earlier work on the synthesis of disordered porous carbons from cyclodextrins, which were components of nanostructured silica/cyclodextrin composites.[78]

Among the aforementioned carbon precursors, those potentially suitable for the synthesis of carbons with graphitic pore walls deserve particular attention. This group includes aromatic and polyaromatic hydrocarbons,[65,66] petroleum and mesophase pitch,[67−71] PAN,[61] and most of the precursors used in carbon CVD processes.[49,72−76] OMCs synthesized from acenaphthene[65] and other aromatic and polyaromatic precursors[66] were already found to have more uniform carbon structures on the atomic level, when compared to those of carbons from sucrose. Also, carbons from aromatic and polyaromatic precursors exhibited enhanced electrical conductivity.[66] PAN is a very promising precursor for nanostructured carbons, because it is known to be an excellent precursor for the synthesis of carbon fibers on commercial scale,[79−81] and was successfully used for the synthesis of highly oriented graphite nanosheets[82] and carbon nanoobjects.[83,84] The use of PAN formed via conventional radical polymerization of acrylonitrile (AN) to prepare carbon nanofilaments in cylindrical mesopores of MCM-41 silica was also explored, and evidence of good electrical conductivity of carbon nanostructures in this silica host was provided, even though the percentage of carbon introduced was low (about 10 wt % in the carbon/silica composite).[85] Recently, a similar approach was used to synthesize OMCs with 2-D hexagonal structure and a strong dependence of the carbon structure on details of PAN stabilization and carbonization conditions was found, whereas the resulting OMCs exhibited moderate specific surface areas and pore volumes.[61]

Herein, it is reported that OMCs and disordered mesoporous carbons can be prepared using ordered and disordered silica templates and PAN as a carbon precursor introduced through a novel method based on surface-initiated atom transfer radical polymerization (ATRP) (see Scheme 1).[86−94] By virtue of using surface-bonded polymerization initiation sites, this novel method confines the introduction of the carbon precursor to the surface of the template, thus mitigating the formation of bulk nontemplated carbon. The obtained OMCs exhibited low microporosity and low secondary mesoporosity, whereas their primary mesopore volumes were very large. Moreover, these carbons had primary mesopore diameters as large as 8−12 nm, whereas most of the OMCs reported to date had much smaller pore diameters. The above properties of our OMCs are highly desirable, yet uncommon for OMCs.

Experimental Details

Reagents. Poly(ethylene oxide)−poly(propylene oxide)−poly(ethylene oxide) triblock copolymer Pluronic P123 ($EO_{20}PO_{70}EO_{20}$, $M_{av} = 5800$ g mol^{-1}) was acquired from BASF. Poly(ethylene oxide)−poly(butylene oxide)−poly(ethylene oxide) triblock copolymer B50-6600 ($EO_{39}BO_{47}EO_{39}$) was ob-

tained from Dow Chemicals. Tetraethyl orthosilicate (TEOS) was acquired from Fluka, and hydrochloric acid, toluene, pyridine, and *N*,*N*-dimethylformamide (DMF) were purchased from Fisher Scientific. Toluene was distilled before use. Trimethylchlorosilane and bpy (2,2′-dipyridyl) were acquired from Acros. Si-150 silica gel was obtained from Aldrich. (3-(Chlorodimethylsilyl)propyl 2-bromoisobutyrate ($Cl-Si(CH_3)_2-[(CH_2)_3-O-CO-C(CH_3)_2Br]$) was prepared according to the procedure described elsewhere.[95] CuCl was purified according to the procedure described by Keller and Wycoff.[96] Acrylonitrile (AN) was passed through a basic alumina column prior to use.

Materials. SBA-15 silica was synthesized in a way similar to that originally reported by Zhao et al.[97] The synthesis mixture composition was 1.0 TEOS:0.0167 P123:5.82 HCl:190 H_2O. The copolymer was dispersed in the HCl solution, and then TEOS was added under vigorous stirring. The mixture was stirred at 313 K for 24 h, and then it was transferred into a Teflon-lined autoclave and heated at 393 K for 1 day. Subsequently, the solid product was filtered, washed with deionized water, and dried. The obtained as-synthesized sample was calcined under nitrogen, which was switched to air at 813 K. The synthesis of FDU-1 silica was carried out as described earlier[98] and is a modification of the original synthesis reported by Yu et al.[99] The synthesis mixture had the following composition: 1 TEOS:0.00735 B50-6600:6 HCl:155 H_2O. The copolymer was dissolved in 2 M HCl and stirred at room temperature to obtain a homogeneous mixture. Then, TEOS was added and the mixture was stirred vigorously in an open container for 1 day at room temperature. Subsequently, the mixture was subjected to a hydrothermal treatment by transferring it to a Teflon-lined autoclave and heating at a temperature of 413 K for 12 h without stirring. The precipitate was filtered out, washed with water, dried at room temperature, and calcined under air at 813 K for 5 h using a heating rate of 5 K min^{-1}.

Surface Modification. The silica was dispersed in toluene (5−25 mL of toluene per 1 g of silica) under magnetic stirring, pyridine was added (toluene/pyridine volume ratio 10:1), and then 3-(chlorodimethylsilyl)propyl 2-bromoisobutyrate was introduced. The amount of the latter reagent was calculated as 2-fold excess with respect to the amount corresponding to the surface coverage of 3 μmol m^{-2} (the latter coverage is an estimate of the maximum surface coverage of organodimethylchlorosilane attainable under the conditions employed herein). The mixture of silica, toluene, pyridine, and silane was heated at 378−383 K for 2 days under magnetic stirring. The product was isolated by filtering and washing several times with toluene and methanol. Then, the sample was dried in a vacuum oven. The obtained samples are denoted X−BiB, where X is the symbol of the silica used. A surface modification with trimethylchlorosilane was carried out in a similar way, but in this case, a larger excess of the silane with respect to the silica was used (toluene/trimethylchlorosilane volume ratio was 5:2) and the modification temperature was 353−358 K. The obtained samples are denoted X−BiB−TMS.

Acrylonitrile Polymerization. AN was polymerized using the ATRP method.[86,87,100−102] The molar ratios of reagents were typically close to BiB/AN/CuCl/bpy = 1:300:1:2, whereas the DMF/AN volume ratio was ∼1.74:1. The polymerization was carried out as follows. The silica with chemically bonded 2-bromoisobutyrate groups and a magnetic stirrer were placed in a Schlenk flask with a septum placed on its arm. The flask was closed with a stopper and the content of the flask was deoxygenated by passing nitrogen gas. 2,2′-Dipyridyl and deoxygenated DMF and AN were added under nitrogen flow, and the mixture was allowed to stir for 5 min. CuCl was then added under nitrogen flow, and the Schlenk flask was placed in an oil bath and heated at 328 K for a selected period of time (2 days for SBA-15, unless noted otherwise; 4 days for FDU-1 and 7 days for Aldrich Si-150). Then, the flask was removed from the heating bath, the stopper was removed, and DMF was added to stop the radical polymerization. Subsequently, the solid product was filtered out, washed with DMF and methanol, and dried in a vacuum oven at 313 K to constant weight. The obtained samples are denoted X−BiB−TMS−PAN.

Carbonization and Isolation of Carbon. The obtained silica/PAN composites were converted to silica/carbon composites through heating under air to 573 K with a heating rate of 2 K min^{-1} to stabilize PAN.[79−81] After reaching 573 K, the air was switched to nitrogen; after an hour, the heating was continued with a rate of 5 K min^{-1} to reach 1073 K, and the latter temperature was maintained for 3 h. The obtained silica/carbon composites are denoted X−BiB−TMS−PAN−SC. The carbon was isolated from the silica matrix through dissolution in 3 M aqueous NaOH solution at 353 K. The alkaline solution was changed four times during the dissolution, which took 1 day. Finally, the carbon sample was washed with water and dried. The carbons are denoted C−X, where X denotes the silica template used.

Characterization. Weight change curves were recorded under air on a TA Instruments TGA 2950 thermogravimetric analyzer in a high-resolution mode with the maximum heating rate of 5 or 10 K min^{-1}. Elemental analysis for carbon and bromine was carried out by Midwest Microlab, LLC (Indianapolis, IN). Nitrogen adsorption measurements at 77 K were performed on ASAP 2010 and 2020 volumetric adsorption analyzers (Micromeritics, Norcross, GA). Before adsorption measurements, the samples were outgassed under vacuum at 473 K. Powder X-ray diffraction (XRD) patterns were recorded on a Philips X'Pert diffractometer operated at 3 kW using Cu Kα radiation. A powder XRD pattern for C−SBA-15 was also acquired at wide angles on a Rigaku Geigerflex diffractometer using Cu Kα radiation. Transmission electron microscopy (TEM) images were recorded using a JEOL 200EX instrument operated at 200 kV. For TEM imaging, samples were dispersed in ethanol and deposited on carbon-coated copper grids.

Calculations. The specific surface area was calculated from nitrogen adsorption data in the relative pressure range from 0.04 to 0.2 using the BET method.[103] The total pore volume was estimated from the amount adsorbed at a relative pressure of 0.99.[103] The micropore volume and the volume of ordered mesopores were calculated for selected carbon samples using the α_s plot method. It should be noted that pores are classified herein according to the IUPAC classification[103] as micropores (width below 2 nm), mesopores (width from 2 to 50 nm), and macropores (width above 50 nm). Nongraphitized carbon black Cabot BP 280 was used as a reference adsorbent in the α_s plot calculations.[104] The micropore volume and the sum of micropore and mesopore volumes were calculated from data in the α_s ranges 0.8−1.0 and 1.85−2.3, respectively. It should be noted that α_s is the standard reduced adsorption defined as the amount adsorbed at a particular relative pressure for the reference adsorbent divided by the amount adsorbed at a relative pressure of 0.4. The pore size distribution was calculated from adsorption branches of isotherms using the Barrett−Joyner−Halenda (BJH) algorithm,[105] the corrected form of the Kelvin equation (calibrated for siliceous cylindrical pores of diameter from 2 to 6.5 nm),[106] and the calibrated statistical film thickness curve for silicas.[107]

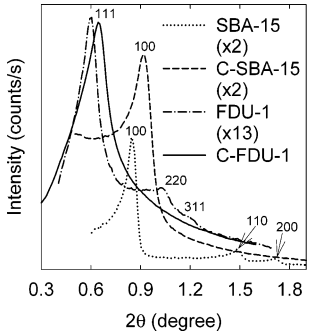

Figure 1. Low-angle XRD patterns for SBA-15 and FDU-1 silicas and mesoporous carbons obtained using these templates (to facilitate the comparison, the intensities were multiplied by factors provided in parentheses).

Results and Discussion

Silica Templates. Three different types of silica templates were selected for this study. One of them was SBA-15 silica with 2-D hexagonally ordered, large (~10 nm), cylindrical mesopores connected with one another through smaller interconnecting pores in the walls of the ordered mesopores.[108] The XRD pattern for this material (Figure 1) featured three pronounced peaks at 2θ angles of 0.845°, 1.48°, and 1.72°, which can be indexed as (100), (110), and (200) reflections of a 2-D hexagonal structure. The (100) interplanar spacing was 10.4 nm, which corresponds to the distance of 12.0 nm between the centers of adjacent mesopores. The second template was FDU-1 silica, whose preparation involved a hydrothermal treatment at high temperature (413 K). The XRD pattern for this silica showed peaks at 2θ angles of 0.60°, 1.02°, and ~1.20° (see Figure 1), which can be indexed as (111), (220), and (311) peaks of face-centered cubic (fcc) structure with a unit-cell parameter of 25 nm. An earlier TEM, electron diffraction, and small-angle X-ray scattering study of an FDU-1 sample synthesized at shorter hydrothermal treatment time (6 h) and lower temperature (373 K) showed that this material had spherical mesopores arranged in fcc arrays with stacking faults characteristic of hexagonal close-packed stacking sequences.[98] The TEM images for the present FDU-1 sample showed projections (data not shown) similar to those observed for the aforementioned FDU-1 sample prepared at lower temperature, although in the present case, there was also some indication of a presence of disordered regions in the material. The third template used in this study was a disordered mesoporous silica gel Si-150.

Shown in Figure 2 are nitrogen adsorption isotherms for the silica templates. The shape of these adsorption isotherms indicates that the adsorption proceeded via monolayer−multilayer formation at relative pressures below 0.7−0.8 (although in cases of SBA-15 and FDU-1, probably there was some contribution from micropore filling at low relative pressures), followed by capillary condensation (complete filling of mesopores) at relative pressures of about 0.8−0.9, after which the isotherms leveled off. The capillary evaporation (emptying of the interior of the mesopore with retention of the multilayer film on its walls) was shifted to lower relative pressures by 0.05 or more with respect to the capillary condensation, giving rise to adsorption−desorption hysteresis, which is a typical adsorption behavior of mesoporous solids. BET specific surface areas, total pore volumes, and pore diameters (that is, maxima on pore size distributions (PSDs) shown in Figure 2) are listed in Table 1. The silica templates exhibited pore diameters from ~11 to 20 nm and BET specific surface areas from 300 to 760 $m^2\ g^{-1}$.

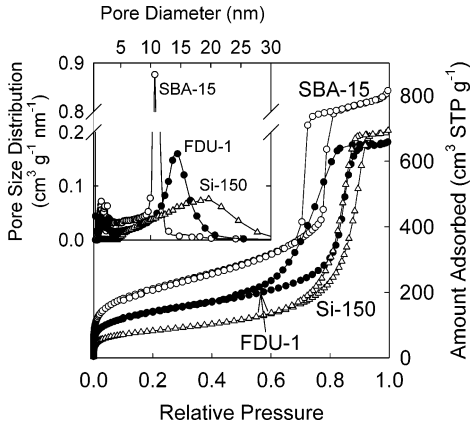

Figure 2. Nitrogen adsorption isotherms and pore size distributions for the silica templates.

TABLE 1: Structural Properties of the Materials under Study

sample	BET specific surface area ($m^2\ g^{-1}$)	total pore volume ($cm^3\ g^{-1}$)	pore diameter (nm)
SBA-15	760	1.25	10.7
SBA-15−BiB−TMS	350	0.65	8.7
SBA-15−BiB−TMS−PAN	20	0.05	
SBA-15−BiB−TMS−PAN−SC	560	0.32	2.4
C−SBA-15	840	1.49	8.4
FDU-1	500	1.01	14.5
FDU-1−BiB−TMS	240	0.60	12.6
FDU-1−BiB−TMS−PAN	<10	0.03	
FDU-1−BiB−TMS−PAN−SC	400	0.30	3.0
C−FDU-1	830	1.75	11.8
Si-150	300	1.06	20
Si-150−BiB−TMS	250	0.85	15
Si-150−BiB−TMS−PAN	40	0.09	*a*
Si-150−BiB−TMS−PAN−SC	350	0.29	*a*
C−Si-150	810	1.77	11

[a] Peak on the borderline between the micropore and mesopore range.

SBA-15 and FDU-1, which are ordered mesoporous silicas, exhibited narrow PSDs, whereas the disordered silica gel Si-150 had a much broader PSD. The total pore volumes of the silica templates were similar and ranged from 1.01 to 1.25 $cm^3\ g^{-1}$.

Introduction of Polymerization Initiation Sites. The modification of the silicas with bromoisobutyrate-containing organosilyl groups (which are hereafter referred to as BiB groups) and trimethylsilyl (TMS) groups led to the introduction of 7.6, 4.2, and 1.2 wt % bromine in the modified materials, which corresponds to the surface coverage of 1.6, 1.3, and 0.53 μmol m^{-2} of BiB groups for SBA-15, FDU-1, and Si-150, respectively. As expected, the pore diameter decreased after the surface modification (see Table 1 and PSDs in Figure 3), which was paralleled by a substantial decrease in pore volume (see Table 1; the decrease in adsorption capacity is seen in Figure 3 for FDU-1 silica). This pore volume decrease can be attributed to two factors. First, the introduction of organic groups decreases the pore diameter and thus the amount of void space in the material. Second, the introduction of organics increases the mass of the sample and thus decreases the pore volume per gram of the sample. Weight percentages of the organic groups chemically bonded to surfaces of the silicas under study were quite significant, as can be seen from the weight losses from about 373 to 900−1100 K (Figure 4), which can be attributed primarily to the burn-out of organic groups. So, the observed decrease in the pore volume after the chemical bonding can be explained

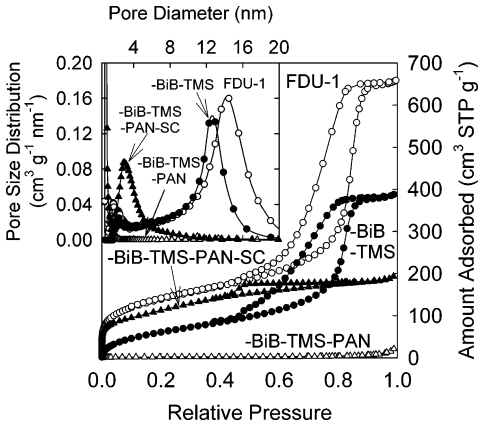

Figure 3. Nitrogen adsorption isotherms and pore size distributions for (i) unmodified FDU-1 silica; (ii) FDU-1 modified with BiB-containing ligands and TMS; (iii) FDU-1/PAN composite, and (iv) FDU-1/carbon composite.

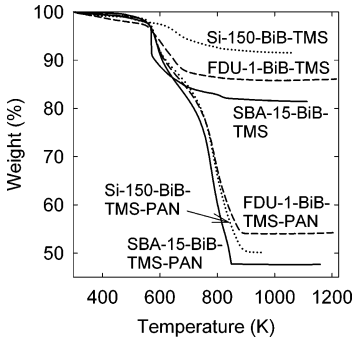

Figure 4. Weight-change curves recorded under air for silica samples with surfaces modified with a layer of polymerization initiation groups and TMS groups, and for the silica/PAN composites obtained after the polymerization.

as an effect of the surface modification with large amounts of organic groups.

Acrylonitrile Polymerization. The surface-initiated polymerization made the mesopores essentially inaccessible to nitrogen at 77 K, as can be inferred from the very low adsorption capacity of the obtained silica/PAN composites (see Table 1 and adsorption isotherm for FDU-1−BiB−TMS−PAN in Figure 3). In principle, the inaccessibility of porosity in silica/PAN composites does not imply that the pores are uniformly infiltrated with the polymer, because the pores may simply be blocked, for instance at the entrances. Weight change patterns under air (Figure 4) allowed us to estimate the actual amount of the organics in the silica/polymer composites and thus the amount of the polymer introduced, which is related to the difference in weight losses for samples before and after polymerization. It can be seen that amounts of the organics in silica/PAN composites, as estimated from the weight loss from ∼373 K to the temperature at which the weight change curves leveled off (∼900 K), were proportional to the total pore volume of the silica templates, which is consistent with our expectation that the AN polymerization took place primarily in the mesopores of the samples rather than on the external surface of their particles. Slightly less than 1 g of organics was introduced per 1 cm^3 of mesopore volume of the template, which is reasonable when one takes into consideration that the expected density of organics in the pores would be about 1 g cm^{-3} in the present case (although the density of PAN is likely to be above 1 g cm^{-3}, the density of surface-bonded initiator groups, and TMS may be appreciably below 1 g cm^{-3}).

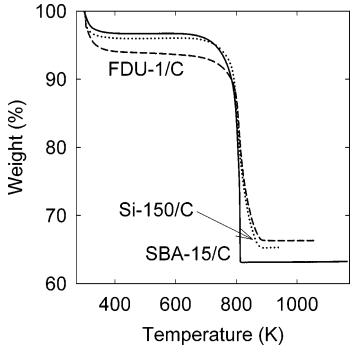

Figure 5. Weight-change curves recorded under air for silica/carbon composites obtained from the silica/PAN composites via stabilization under air and carbonization under nitrogen.

Stabilization and Carbonization. As illustrated in Figure 3 for the FDU-1 silica, the stabilization and carbonization of PAN brought about an increase in the adsorption capacity. This can be understood when one considers structural changes that are expected to take place during these processes. First, PAN is converted to carbon. It is known that the yield of carbon from stabilized PAN is typically about 60 wt %.[79] Moreover, the density of PAN (which is ∼1.18 g cm^{-3}) is lower than the density of carbon (carbon fibers from PAN have density in the range from 1.5 to 2.0 g cm^{-3}).[79−81] This suggests that the conversion of PAN to carbon is accompanied by a significant volume decrease (by the factor of 2−3), provided the carbon framework formed from PAN does not have internal microporous voids. This assumption seems to be a good approximation, as our carbons from PAN exhibit small amount of micropores. It also needs to be kept in mind that the surface-bonded ATRP initiator groups (more specifically, $-Si(CH_3)_2-[(CH_2)_3-O-CO-C(CH_3)_2-]$ groups, which are connected to the PAN chains and from which bromine was transferred during the initiation of the polymerization), and $-Si(CH_3)_3$ groups are likely to decompose during the stabilization and/or carbonization, although some amount of carbon from these groups may be retained. As can be inferred from the weight change curves recorded under air for silica/PAN composites (Figure 4) and silica/carbon composites (Figure 5), the amount of combustible matter (that is, organics before and carbonaceous material after the stabilization and carbonization) per unit mass of silica decreased by the factor of about 2 as a result of stabilization and carbonization. Both the decrease in mass and increase in density are expected to contribute to a substantial decrease in the volume of the carbon-containing matter in the pores of the silica templates. On the other hand, the mesopore volume of the silica template is expected to decrease in the course of the thermal treatment employed during the carbonization, as inferred from earlier studies of thermal behavior of ordered mesoporous silicas.[108,109] The fact that the silica/carbon composites had appreciable adsorption capacities suggests that the decrease in volume related to the contraction of the carbon precursor (and other organics present in the pores) upon the conversion to carbon was more significant than the decrease in volume of voids in the silica framework upon heating to 1073 K. The silica/carbon composites discussed here did not exhibit any appreciable mesoporosity of size comparable to that observed for the silica templates (see PSD in Figure 3). This suggests that the mesopores of these templates were uniformly filled with carbon. It should be noted that shorter polymerization times (for instance, less than 1 day for SBA-15/PAN samples), which were not sufficient to completely fill the mesopores of the silica templates with PAN, afforded silica/PAN composites, whose conversion

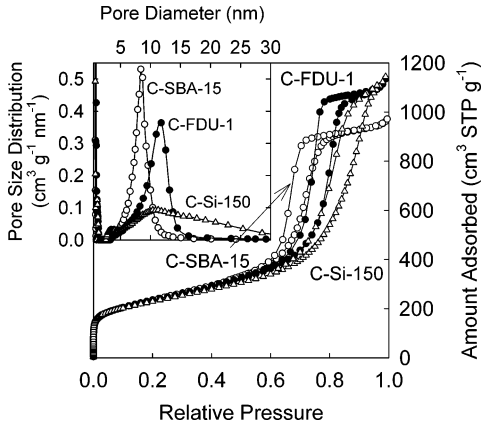

Figure 6. Nitrogen adsorption isotherms and pore size distributions for the templated mesoporous carbons derived from PAN.

to silica/carbon composites resulted in the occurrence of mesopores of size similar to that of the mesopores of the template (see adsorption isotherms shown in Supporting Information, Figure 1S). This behavior indicates that there was a significant inhomogeneity in the distribution of carbon in the mesopores of the templates. It is also noteworthy that the percentages of carbon in silica/carbon composites, which amounted to 28−34 wt %, were somewhat lower than those typically observed for silica/carbon composites used as precursors for the synthesis of ordered mesoporous carbons.[110,111] In the case of inverse replication, a low content of the component that forms the replica in the template/replica composite implies high pore volume for the replica, as long as the latter does not collapse upon removal of the template. This is because, in such a case, the porosity of the inverse replica consists of the space once occupied by the template and any space between the template and the replica. On the basis of this reasoning, a relatively low content of carbon in the silica/carbon composites is likely to be the primary source of the very large mesopore volume of OMCs obtained using the present method (see below).

Mesoporous Carbons. Nitrogen adsorption isotherms for the obtained mesoporous carbons and the corresponding PSDs are shown in Figure 6. The total pore volumes, specific surface areas, and mesopore diameters (estimated from the positions of PSD maxima) are provided in Table 1. All carbons exhibited very high adsorption capacity (total pore volume of 1.5−1.8 $cm^3\ g^{-1}$), although their BET specific surface areas were moderate (700−840 $m^2\ g^{-1}$). Silica-templated mesoporous carbons synthesized using other methods often exhibit specific surface areas significantly above 1000 $m^2\ g^{-1}$, but this is largely due to the fact that these carbons are typically significantly microporous, whereas our materials have relatively low microporosity (as discussed below). The carbons templated by SBA-15 and FDU-1 silicas exhibited narrow PSDs, whereas PSD for the carbon templated by the disordered silica (Si-150) was broader, which may be due to a wide range of wall thicknesses in this template. The pore size of C−SBA-15 (∼8 nm) is significantly larger than the pore sizes of typical carbon replicas of SBA-15 (∼5 nm).[50] This can be understood when one takes into account that, in the typical OMC synthesis, a carbon precursor can fill the entire mesopore structure of the silica template, and thus OMC pore size is primarily determined by the thickness of the pore walls of the template. In our case, the presence of a layer of polymerization initiation groups (∼1 nm thickness) on the template surface reduces the space that is filled with the carbon precursor and increases the distance between the elements of the carbon framework formed, thus affording the OMC with larger mesopores.

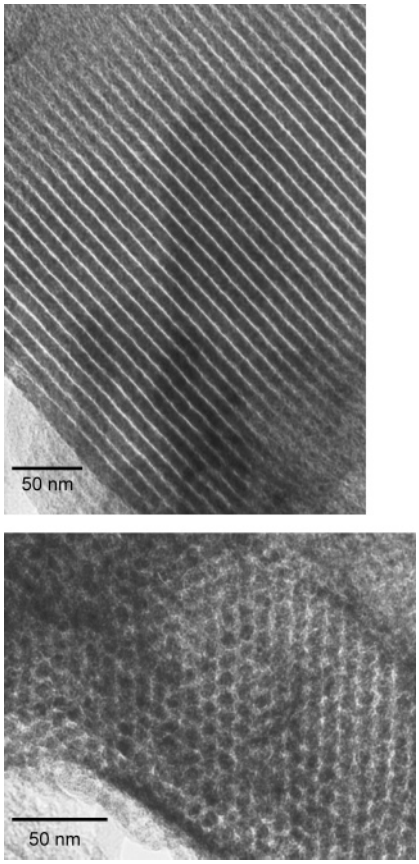

Figure 7. TEM images of carbon templated by SBA-15 silica.

TEM images of C−SBA-15 show large areas of parallel stripes (Figure 7, top). These stripes can be interpreted as images of carbon nanorods aligned perpendicular to the electron beam. The stripes tend to have nearly constant thickness, pointing to uniform diameters of nanorods. Hexagonal arrangements of closely spaced dots visible in some parts of the images can be regarded as projections of the carbon nanorods aligned parallel to the electron beam (Figure 7, bottom). An XRD pattern for C−SBA-15 carbon consisted of a single peak centered at the 2θ angle of 0.92° (see Figure 1), which corresponds to a d spacing of 9.6 nm. On the basis of the TEM evidence of hexagonal packing for C−SBA-15 and the XRD patterns of its SBA-15 template, the single peak in the XRD pattern of C−SBA-15 can be indexed as (100) reflection of a 2-D hexagonal structure. Notably, the (100) interplanar spacing of the inverse replica was ∼8% smaller than that of the template. According to the literature evidence, the packing of carbon nanorods in the replicas of SBA-15 silicas can range from 2-D hexagonally ordered arrays (these materials were originally denoted CMK-3)[50] to disordered structures,[112,113] depending on the amount of pores forming interconnections between the primary (ordered) mesopores in the silica template[112] and on the extent of infiltration of these interconnections with the carbon precursor. Although the SBA-15 silica template used in this study was synthesized under conditions favoring interconnections,[50,114] the surface modification with rather large BiB-containing organic groups could block and/or decrease the size of the considerable fraction of these connections.[108] To elucidate the presence of connections in the SBA-15 structure, one can consider whether the structural parameters, such as the specific surface area, pore volume, and primary mesopore diameter for

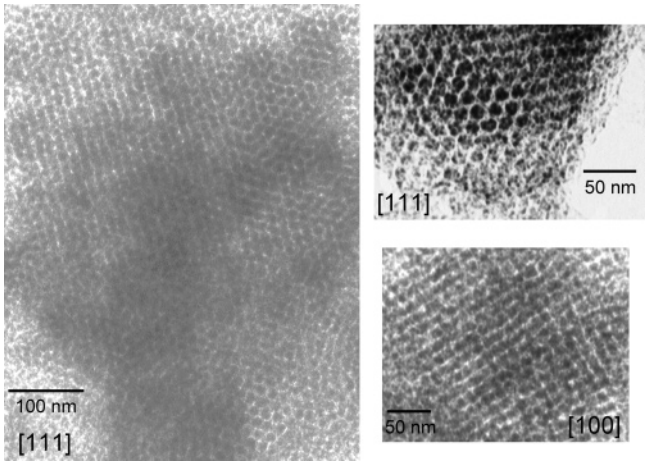

Figure 8. TEM images of carbon templated by FDU-1 silica.

a given sample, fulfill a relation for uniform cylindrical mesopores.[108,112] In the case of ideal cylindrical pores, the pore diameter (*w*) multiplied by the specific surface area (*S*) and divided by the pore volume (*V*), *wS/V*, is equal to 4. Experimental *wS/V* values for uniform cylindrical mesopores of silicas were typically about 4.6, and the deviations from the theoretical value of 4.0 was attributed to the overestimation of the specific surface area using the BET method.[112] For the SBA-15 silica template used herein, *wS/V* was equal to 6.5 (the calculations of *S* and *V* values are described elsewhere[108]), which is common for SBA-15 silicas and indicative of the presence of small pores, which are located in the walls of the ordered cylindrical mesopores, and provide connectivity between the latter. These small pores significantly contribute to the surface area (the numerator in *wS/V*) and contribute to a smaller extent to the pore volume (the denominator in *wS/V*), which makes *wS/V* larger than the value characteristic of cylindrical pores. For our organic-modified SBA-15−BiB−TMS sample, the *wS/V* value was 4.5, which was only slightly higher than $wS/V = 4.2$ for SBA-15 sample modified with high content of large organic groups, which effectively close the connecting pores. These results suggest that the connecting pores were significantly depleted in SBA-15−BiB−TMS sample. Consequently, low connectivity between the carbon rods that form the inverse replica of SBA-15 is expected and thus the replica may exhibit some propensity for distortions, for example, tilt of adjacent nanorods with respect to one another. Such a distortion was indeed observed by TEM (image not shown), although in a very small area; more importantly, distortions of this kind may account for the absence of higher-order peaks in the XRD pattern (Figure 1). Regardless, the carbon replica of SBA-15 described here can be classified as OMC of CMK-3 type.

TEM images for the carbon inverse replica of FDU-1 silica revealed the presence of ordered domains of an appreciable size. Shown in Figure 8 are projections that can be identified as [111] and [100] projections of face-centered cubic structure. Projections that look like patterns of parallel stripes were also observed, as in the case of FDU-1 silicas. Some of these stripes appeared to be clearly modulated or composed of spheres (images not shown). It can be easily demonstrated that such patterns can be produced when a cubic close-packed array of spheres is viewed at a slight tilt (for instance, [100] projection with tilt of 5−10 degrees). The XRD pattern of the C−FDU-1 carbon featured a single strong peak with a maximum at 0.65° (see Figure 1), which corresponds to an interplanar spacing of 13.6 nm. The peak was slightly broader than the main peak of the FDU-1 template. It should be noted that the (100) peak of the C−SBA-15 was also broader than that of the SBA-15 template (see Figure 1). It should be emphasized that the carbon inverse replica (synthesized by others using sucrose as a carbon precursor) of silica structurally similar to FDU-1 featured very broad XRD peaks, when compared to those observed on the XRD pattern for its template.[52] In our case, the inverse replication appeared to better preserve the nanostructure of the template, and it also afforded a carbon with a higher pore volume.

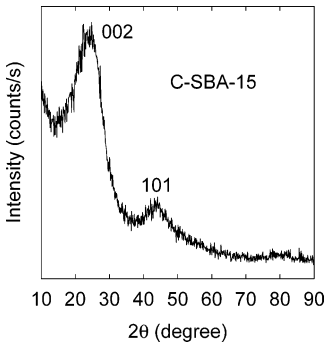

Figure 9. Wide-angle XRD pattern for an SBA-15-templated mesoporous carbon derived from PAN (data collected on a Rigaku Geigerflex diffractometer).

TEM allowed us to gain some insight into the structure of C−Si-150 carbon, as the TEM images (Supporting Information, Figure 2S) showed the presence of disordered porosity of diameter similar to that inferred from the PSD assessed from nitrogen adsorption data.

A wide-angle powder XRD pattern of a carbon replica of SBA-15 is shown in Figure 9. It features a strong peak centered at ∼24° (which corresponds to the interplanar spacing of ∼0.37 nm) and a less intense peak at ∼44°. These peaks can be identified as (002) and (101) peaks of a graphitic carbon structure.[65] OMCs obtained from sucrose, which is the most common precursor for the synthesis of OMCs, exhibit XRD patterns with no clear (002) peak,[65] even after heating at 1673 K,[67] although a shoulder at 2θ angles of 20−25° can be observed. However, OMCs from some other carbon precursors, namely, polyaromatic and aromatic hydrocarbons,[65,66] poly(vinyl chloride), PVC,[63] pitch,[67,71] and propylene,[68] acetonitrile,[75,76] and styrene,[75] were reported to exhibit pronounced (002) peaks on their XRD patterns, which was in many cases regarded as evidence for their appreciable ordering on atomic scale. Our carbons were subjected to heat treatment at only 1073 K, and consequently, a further improvement of the ordering on atomic scale can be expected when higher carbonization temperature is used or the carbon liberated from the template is subjected to a heat treatment at a temperature above 1073 K.

As expected for materials obtained from the PAN precursor, the carbons described herein contained an appreciable amount of nitrogen. The C/N molar ratio for C−SBA-15 was 7.4:1, and the C/H ratio was 3.1:1. These results are similar to those for other carbons derived from PAN and carbonized at comparable temperatures.[61,115]

Influence of the Amount of Carbon Precursor on the Structure of SBA-15-Templated Carbon. The amount of PAN in SBA-15/PAN composites was found to appreciably affect the structure of the carbon inverse replica. The SBA-15/PAN composites obtained after 1−2 days of polymerization, which had the content of organics corresponding to the maximum filling of the initiator-modified mesopores with PAN, yielded carbon replicas with narrow PSDs and high total pore volumes (1.4−1.5 $cm^3\ g^{-1}$). However, lower degrees of infiltration with

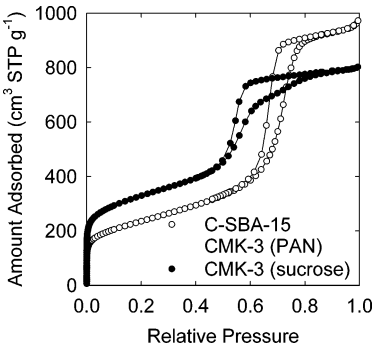

Figure 10. Comparison of nitrogen adsorption isotherms for inverse replicas of SBA-15 prepared from PAN (present approach) and from sucrose.[112]

PAN (1/2 to 2/3 of maximum PAN loading achieved after 2−4 h of polymerization) afforded carbons with lower quality, and for a very low PAN infiltration level (∼1/3 of maximum loading), the obtained carbon almost did not feature any capillary condensation step on its adsorption isotherm (see Supporting Information, Figure 3S). These lower-quality carbons had broader PSDs and reduced total pore volumes, although their specific surface areas were comparable or even higher than those for the most uniform SBA-15-templated carbons obtained in cases where the PAN infiltration of the template was essentially complete. One of these lower-quality carbons (obtained after the polymerization time of 4 h) was imaged by TEM and found to feature areas with apparently discontinuous or undulating rods, which were aligned parallel to one another (see Supporting Information, Figure 4S). Perhaps the loss of continuity of carbon nanorods led to a local structural collapse, thus reducing the pore size uniformity and pore diameter of these carbons. Another evidence of the loss of continuity of the carbon nanorods is the adsorption behavior of SBA-15/C composites obtained from SBA-15/PAN composites with lower PAN contents (see Supporting Information, Figure 1S). In the case of these SBA-15/C composites, there was evidence of accessible, uniform porosity of diameter about 8 nm (∼2.5 nm smaller than the pore diameter of the SBA-15 template). The SBA-15 silica framework shrunk upon heating to 1073 K (which is employed during carbonization), and an additional monolayer or submonolayer of silica was introduced on the SBA-15 surface as a result of its modification with the organosilanes. Therefore, these uniform mesopores in the SBA-15/carbon composites are likely to be parts of mesopores of the SBA-15 template, which were not filled with any appreciable amount of carbon. The volume of these uniform voids increased as the degree of infiltration with PAN decreased. This indicates that upon PAN stabilization/carbonization, there was a tendency for the formation of discontinuous carbon nanorods of constant diameter.

Advantages of the Present Method for Mesoporous Carbon Synthesis. The method for the synthesis of OMCs described herein has several attractive features. The volume of uniform mesopores of the obtained carbons is very high in comparison to that of other OMCs, except for those with tube-like structures.[3,111] Shown in Figure 10 is the comparison of adsorption isotherms for the SBA-15-templated (CMK-3 type) carbons obtained from PAN using the present method, and from sucrose (data taken from an earlier work[112]). One can immediately notice that the amount adsorbed below the onset of capillary condensation step was much lower and the capillary condensation step was much higher for the carbon synthesized using the present method. This implies that the specific surface area of the carbon prepared via the present method was significantly lower, whereas the volume of ordered mesopores was much higher. In fact, the specific surface areas estimated using the BET method were 840 and 1160 m^2 g^{-1} for the carbons from PAN and sucrose, respectively. This difference is mostly attributable to the fact that the carbon from PAN had a relatively very low micropore volume (0.07 cm^3 g^{-1}), which was almost three times lower than that of the carbon from sucrose (0.19 cm^3 g^{-1}); therefore, in the former case, the surface area of micropores was much lower. On the other hand, the volume of uniform mesopores was about 1.26 cm^3 g^{-1} for the carbon from PAN, whereas it was below 0.94 cm^3 g^{-1} for the carbon from sucrose (in this case, the exact value is difficult to evaluate, as the adsorption isotherm did not level off after the completion of the capillary condensation in the uniform mesopores, indicating the presence of mesoporous defects). Similar conclusions can be made when one compares the adsorption data for C−FDU-1 with those for carbons with similar structures reported earlier.[52] So, the use of PAN afforded the mesoporous carbon with low microporosity and a very high mesopore volume. Recently, the use of other carbon precursors that are suitable for the formation of carbons with low microporosity was explored. These carbon precursors included aromatic (usually polyaromatic) hydrocarbons,[65,66] mesophase pitch,[69,71] and petroleum pitch.[67] However, these carbons exhibited relatively low volumes of uniform mesopores (0.3−0.6 cm^3 g^{-1}) and small mesopore diameters. A carbon inverse replica of SBA-15 synthesized using PAN infiltration via uncontrolled radical polymerization, as reported by others,[61] also had a very low mesopore volume. In some cases, these low pore volumes may be partially due to the presence of domains of nontemplated carbon,[68] but an important common cause of the low pore volume may be a high content of carbon in the silica/carbon composites formed using these methods, which results in low volumes of void space per gram of inverse carbon replica. So, the present OMCs combine a very high mesopore volume with low microporosity, low secondary (defective) mesoporosity, and a certain degree of the atomic-scale ordering, which is a combination of properties that has not been reported before.

Another attractive feature of our carbon infiltration procedure is that the introduction of the carbon precursor is confined to the surface of the silica template. Thus, the formation of bulk carbon, which was reported to take place in some other important methods of ordered mesoporous carbon synthesis (those based on CVD,[49] and infiltration with petroleum pitch),[67] is mitigated. The synthesis of ordered mesoporous carbons using mesophase pitch may also be prone to the formation of some amount of nontemplated carbon.[69] In the case of many other carbon infiltration procedures, the lack of formation of nontemplated carbon is also difficult to ensure, except for the cases where the formation of carbon or polymeric carbon precursor takes place on particular surface sites (for example, aluminum heteroatoms in cases of polymerization of phenol and formaldehyde[2] or furfuryl alcohol[3]). In the case of the present method, there is a chance of the formation of a somewhat thicker carbon framework on the surface of particles than in the mesopores of the template. This supposition is supported by TEM data. As can be seen in Figure 7, top image, the parallel stripes have uniform width, except for the outermost one, which is somewhat wider. This may be due to the fact that the AN polymerization in the mesopores of the template is constricted by the available pore volume and is suppressed once the pores are essentially completely filled with PAN, whereas the polymerization on the external surface of particles of the template is not subject to these spatial constraints. However, the controlled nature of the

surface-initiated polymerization process used here allows one to avoid the formation of a thick, nonuniform coat of carbon on the external surface of particles. This is supported by the observation that the aforementioned wider stripe, which can be regarded as an image of the carbon layer on the exterior of the particle, is very uniform in width and only slightly thicker than the templated carbon framework. In many other methods for the synthesis of ordered mesoporous carbons, the amount of carbon introduced into the silica template is controlled by the amount of the carbon precursor used for the synthesis. This may be a serious limitation in cases where silica templates are in the form of thin films and thus the needed amount of carbon precursor is small and its uniform introduction into the mesopores of the template would be very difficult. Perhaps this is a reason why we are aware of only one report on the formation of a mesoporous carbon film using ordered mesoporous silica as a template.[3] In the present method, the monomer is introduced in excess and its conversion into surface-bonded carbon precursor (PAN) is spatially uniform from its principle and is controlled by the polymerization conditions. This makes the present method particularly suitable for the preparation of thin films of mesoporous carbon using mesoporous silica films as templates.

Conclusions

PAN is an excellent precursor for the synthesis of OMCs, giving rise to semi-graphitic materials with high mesopore volume, large mesopore diameter, relatively low microporosity, low secondary mesoporosity, and some extent of graphitic ordering in the carbon framework. The OMCs obtained after carbonization at 1073 K contain an appreciable amount of nitrogen. The surface-initiated polymerization allows one to confine the introduction of the carbon precursor to the surface of the template, which mitigates the formation of bulk nontemplated carbon. In the case of the synthesis method described herein, there is an appreciable weight loss during the stabilization and carbonization, which is related to the inherent properties of PAN precursor and also to the decomposition of the polymerization initiator groups and TMS groups. Importantly, this weight loss is not accompanied by the creation of any appreciable amounts of micropores. The carbon content in silica/carbon composites obtained from silica/PAN composites with maximum PAN loading is relatively low, but the carbon nanostructure is stable upon the silica template removal. Because of the high proportion of the silica to carbon, the removal of silica creates very high primary mesopore volume. The extent of infiltration of the surface-modified silica template with PAN has a significant influence on the pore size uniformity and mesopore volume of the ordered carbon obtained using SBA-15 template. A high degree of infiltration leads to carbons of the highest quality.

Acknowledgment. The support from NSF Grant DMR-0304508 is gratefully acknowledged. K.M. also acknowledges support from NSF Grant DMR-0090409. Noel T. Nuhfer is acknowledged for assistance in TEM analysis. Jason Wolf is acknowledged for assistance in powder XRD analysis.

Supporting Information Available: Four figures: 2 figures with experimental TEM images, and 2 figures with experimental gas adsorption data. This material is available free of charge via the Internet at http://pubs.acs.org.

References and Notes

(1) Ryoo, R.; Joo, S. H.; Jun, S. *J. Phys. Chem. B* **1999**, *103*, 7743.
(2) Lee, J.; Yoon, S.; Hyeon, T.; Oh, S. M.; Kim, K. B. *Chem. Commun.* **1999**, 2177.
(3) Joo, S. H.; Choi, S. J.; Oh, I.; Kwak, J.; Liu, Z.; Terasaki, O.; Ryoo, R. *Nature* **2001**, *412*, 169.
(4) Han, S.; Hyeon, T. *Carbon* **1999**, *37*, 1645.
(5) Han, S.; Hyeon, T. *Chem. Commun.* **1999**, 1955.
(6) Kawashima, D.; Aihara, T.; Kobayashi, Y.; Kyotani, T.; Tomita, A. *Chem. Mater.* **2000**, *12*, 3397.
(7) Li, Z.; Jaroniec, M. *J. Am. Chem. Soc.* **2001**, *123*, 9208.
(8) Li, Z.; Jaroniec, M. *Carbon* **2001**, *39*, 2080.
(9) Ryoo, R.; Joo, S. H.; Kruk, M.; Jaroniec, M. *Adv. Mater.* **2001**, *13*, 677.
(10) Lee, K. T.; Oh, S. M. *Chem. Commun.* **2002**, 2722.
(11) Lukens, W. W.; Stucky, G. D. *Chem. Mater.* **2002**, *14*, 1665.
(12) Taguchi, A.; Smatt, J.-H.; Linden, M. *Adv. Mater.* **2003**, *15*, 1209.
(13) Lee, J.; Han, S.; Hyeon, T. *J. Mater. Chem.* **2004**, *14*, 478.
(14) Shi, Z.-G.; Feng, Y.-Q.; Xu, L.; Da, S.-L.; Zhang, M. *Carbon* **2004**, *42*, 1677.
(15) Han, S.; Sohn, K.; Hyeon, T. *Chem. Mater.* **2000**, *12*, 3337.
(16) Vinu, A.; Streb, C.; Murugesan, V.; Hartmann, M. *J. Phys. Chem. B* **2003**, *107*, 8297.
(17) Choi, M.; Ryoo, R. *Nature Mater.* **2003**, *2*, 473.
(18) Ahn, W. S.; Min, K. I.; Chung, Y. M.; Rhee, H. K.; Joo, S. H.; Ryoo, R. *Stud. Surf. Sci. Catal.* **2001**, *135*, 4710.
(19) Yang, H.; Shi, Q.; Liu, X.; Xie, S.; Jiang, D.; Zhang, F.; Yu, C.; Tu, B.; Zhao, D. *Chem. Commun.* **2002**, 2842.
(20) Yoon, S.; Lee, J.; Hyeon, T.; Oh, S. M. *J. Electrochem. Soc.* **2000**, *147*, 2507.
(21) Lee, J.; Kim, J.; Lee, Y.; Yoon, S.; Oh, S. M.; Hyeon, T. *Chem. Mater.* **2004**, *16*, 3323.
(22) Lee, J.; Yoon, S.; Oh, S. M.; Shin, C.-H.; Hyeon, T. *Adv. Mater.* **2000**, *12*, 359.
(23) Zhou, H.; Zhu, S.; Hibino, M.; Honma, I. *J. Power Sources* **2003**, *122*, 219.
(24) Furukawa, H.; Hibino, M.; Zhou, H.-S.; Honma, I. *Chem. Lett.* **2003**, *32*, 132.
(25) Vix-Guterl, C.; Saadallah, S.; Jurewicz, K.; Frackowiak, E.; Reda, M.; Parmentier, J.; Patarin, J.; Beguin, F. *Mater. Sci. Eng. B* **2004**, *B108*, 148.
(26) Jurewicz, K.; Vix-Guterl, C.; Frackowiak, E.; Saadallah, S.; Reda, M.; Parmentier, J.; Patarin, J.; Beguin, F. *J. Phys. Chem. Solids* **2004**, *65*, 287.
(27) Chai, G. S.; Yoon, S. B.; Yu, J.-S.; Choi, J.-H.; Sung, Y.-E. *J. Phys. Chem. B* **2004**, *108*, 7074.
(28) Chan, K.-Y.; Ding, J.; Ren, J.; Cheng, S.; Tsang, K. Y. *J. Mater. Chem.* **2004**, *14*, 505.
(29) Zhou, H.; Zhu, S.; Hibino, M.; Honma, I.; Ichihara, M. *Adv. Mater.* **2003**, *15*, 2107.
(30) Long, J. W.; Dunn, B.; Rolison, D. R.; White, H. S. *Chem. Rev.* **2004**, *104*, 4463.
(31) Li, Z.; Jaroniec, M. *Anal. Chem.* **2004**, *76*, 5479.
(32) Sakthivel, A.; Huang, S.-J.; Chen, W.-H.; Lan, Z.-H.; Chen, K.-H.; Kim, T.-W.; Ryoo, R.; Chiang, A. S. T.; Liu, S.-B. *Chem. Mater.* **2004**, *16*, 3168.
(33) Kang, M.; Yi, S. H.; Lee, H. I.; Yie, J. E.; Kim, J. M. *Chem. Commun.* **2002**, 1944.
(34) Lu, A.-H.; Schmidt, W.; Taguchi, A.; Spliethoff, B.; Tesche, B.; Schuth, F. *Angew. Chem., Int. Ed.* **2002**, *41*, 3489.
(35) Parmentier, J.; Vix-Guterl, C.; Saadallah, S.; Reda, M.; Illescu, M.; Werckmann, J.; Patarin, J. *Chem. Lett.* **2003**, *32*, 262.
(36) Kim, J. Y.; Yoon, S. B.; Yu, J.-S. *Chem. Mater.* **2003**, *15*, 1932.
(37) Kim, S.-S.; Shah, J.; Pinnavaia, T. J. *Chem. Mater.* **2003**, *15*, 1664.
(38) Lamond, T. G.; Marsh, H. *Carbon* **1964**, *1*, 281.
(39) Hu, Z. H.; Srinivasan, M. P.; Ni, Y. M. *Adv. Mater.* **2000**, *12*, 62.
(40) Kyotani, T. *Carbon* **2000**, *38*, 269.
(41) Pekala, R. W.; Alviso, C. T.; Kong, F. M.; Hulsey, S. S. *J. Non-Cryst. Solids* **1992**, *145*, 90.
(42) Tamon, H.; Ishizaka, H.; Yamamoto, T.; Suzuki, T. *Carbon* **2000**, *38*, 1099.
(43) Knox, J. H.; Kaur, B.; Millward, G. R. *J. Chromatogr.* **1986**, *352*, 3.
(44) Iijima, S. *Nature* **1991**, *354*, 56.
(45) Ross, P.; Knox, J. H. *Adv. Chromatogr.* **1997**, *37*, 121.
(46) Beck, J. S.; Vartuli, J. C.; Roth, W. J.; Leonowicz, M. E.; Kresge, C. T.; Schmitt, K. D.; Chu, C. T. W.; Olson, D. H.; Sheppard, E. W.; et al. *J. Am. Chem. Soc.* **1992**, *114*, 10834.
(47) Yanagisawa, T.; Shimizu, T.; Kuroda, K.; Kato, C. *Bull. Chem. Soc. Jpn.* **1990**, *63*, 988.
(48) Inagaki, S.; Fukushima, Y.; Kuroda, K. *J. Chem. Soc., Chem. Commun.* **1993**, 680.
(49) Kaneda, M.; Tsubakiyama, T.; Carlsson, A.; Sakamoto, Y.; Ohsuna, T.; Terasaki, O.; Joo, S. H.; Ryoo, R. *J. Phys. Chem. B* **2002**, *106*, 1256.
(50) Jun, S.; Joo, S. H.; Ryoo, R.; Kruk, M.; Jaroniec, M.; Liu, Z.; Ohsuna, T.; Terasaki, O. *J. Am. Chem. Soc.* **2000**, *122*, 10712.

(51) Ryoo, R.; Joo, S. H.; Jun, S.; Tsubakiyama, T.; Terasaki, O. *Stud. Surf. Sci. Catal.* **2001**, *135*, 1121.
(52) Fan, J.; Yu, C.; Gao, F.; Lei, J.; Tian, B.; Wang, L.; Luo, Q.; Tu, B.; Zhou, W.; Zhao, D. *Angew. Chem., Int. Ed.* **2003**, *42*, 3146.
(53) Lee, J.; Sohn, K.; Hyeon, T. *J. Am. Chem. Soc.* **2001**, *123*, 5146.
(54) Yoon, S. B.; Sohn, K.; Kim, J. Y.; Shin, C.-H.; Yu, J.-S.; Hyeon, T. *Adv. Mater.* **2002**, *14*, 19.
(55) Fuertes, A. B.; Nevskaia, D. M. *J. Mater. Chem.* **2003**, *13*, 1843.
(56) Lu, A.-H.; Schmidt, W.; Spliethoff, B.; Schueth, F. *Adv. Mater.* **2003**, *15*, 1602.
(57) Che, S.; Garcia-Bennett, A. E.; Liu, X.; Hodgkins, R. P.; Wright, P. A.; Zhao, D.; Terasaki, O.; Tatsumi, T. *Angew. Chem., Int. Ed.* **2003**, *42*, 3930.
(58) Yoon, S. B.; Kim, J. Y.; Yu, J.-S. *Chem. Commun.* **2001**, 559.
(59) Yoon, S. B.; Kim, J. Y.; Yu, J.-S. *Chem. Commun.* **2002**, 1536.
(60) Moriguchi, I.; Koga, Y.; Matsukura, R.; Teraoka, Y.; Kodama, M. *Chem. Commun.* **2002**, 1844.
(61) Lu, A.; Kiefer, A.; Schmidt, W.; Schueth, F. *Chem. Mater.* **2004**, *16*, 100.
(62) Lu, A.-H.; Schmidt, W.; Matoussevitch, N.; Bonnemann, H.; Spliethoff, B.; Tesche, B.; Bill, E.; Kiefer, W.; Schuth, F. *Angew. Chem., Int. Ed.* **2004**, *43*, 4303.
(63) Fuertes, A. B.; Alvarez, S. *Carbon* **2004**, *42*, 3049.
(64) Fuertes, A. B.; Nevskaia, D. M. *Microporous Mesoporous Mater.* **2003**, *62*, 177.
(65) Kim, T.-W.; Park, I.-S.; Ryoo, R. *Angew. Chem., Int. Ed.* **2003**, *42*, 4375.
(66) Kim, C. H.; Lee, D.-K.; Pinnavaia, T. J. *Langmuir* **2004**, *20*, 5157.
(67) Vix-Guterl, C.; Saadallah, S.; Vidal, L.; Reda, M.; Parmentier, J.; Patarin, J. *J. Mater. Chem.* **2003**, *13*, 2535.
(68) Parmentier, J.; Saadhallah, S.; Reda, M.; Gibot, P.; Roux, M.; Vidal, L.; Vix-Guterl, C.; Patarin, J. *J. Phys. Chem. Solids* **2004**, *65*, 139.
(69) Li, Z.; Jaroniec, M. *J. Phys. Chem. B* **2004**, *108*, 824.
(70) Li, Z.; Del Cul, G. D.; Yan, W.; Liang, C.; Dai, S. *J. Am. Chem. Soc.* **2004**, *126*, 12782.
(71) Yang, H.; Yan, Y.; Liu, Y.; Zhang, F.; Zhang, R.; Meng, Y.; Li, M.; Xie, S.; Tu, B.; Zhao, D. *J. Phys. Chem. B* **2004**, *108*, 17320.
(72) Vix-Guterl, C.; Boulard, S.; Parmentier, J.; Werckmann, J.; Patarin, J. *Chem. Lett.* **2002**, 1062.
(73) Zhang, W.-H.; Liang, C.; Sun, H.; Shen, Z.; Guan, Y.; Ying, P.; Li, C. *Adv. Mater.* **2002**, *14*, 1776.
(74) Xia, Y.; Mokaya, R. *Adv. Mater.* **2004**, *16*, 886.
(75) Xia, Y.; Mokaya, R. *Adv. Mater.* **2004**, *16*, 1553.
(76) Xia, Y.; Yang, Z.; Mokaya, R. *J. Phys. Chem. B* **2004**, *108*, 19293.
(77) Kim, J.; Lee, J.; Hyeon, T. *Carbon* **2004**, *42*, 2711.
(78) Han, B.-H.; Zhou, W.; Sayari, A. *J. Am. Chem. Soc.* **2003**, *125*, 3444.
(79) Chung, D. D. L. *Carbon fiber composites*; Butterworth-Heinemann: Newton, 1994.
(80) Peebles, L. H. *Carbon fibers: formation, structure, and properties*; CRC Press: Boca Raton, FL, 1995.
(81) *Carbon fibers*; 3rd ed.; Donnet, J.-B., Wang, T. K., Rebouillat, S., Peng, J. C. M., Eds.; Marcel Dekker: New York, 1998.
(82) Kyotani, T.; Sonobe, N.; Tomita, A. *Nature* **1988**, *331*, 331.
(83) Kowalewski, T.; Tsarevsky, N. V.; Matyjaszewski, K. *J. Am. Chem. Soc.* **2002**, *124*, 10632.
(84) Tang, C.; Qi, K.; Wooley, K. L.; Matyjaszewski, K.; Kowalewski, T. *Angew. Chem., Int. Ed.* **2004**, *43*, 2783.
(85) Wu, C.-G.; Bein, T. *Science* **1994**, *266*, 1013.
(86) Wang, J.-S.; Matyjaszewski, K. *J. Am. Chem. Soc.* **1995**, *117*, 5614.
(87) Matyjaszewski, K.; Xia, J. *Chem. Rev.* **2001**, *101*, 2921.
(88) Kowalewski, T.; McCullough, R. D.; Matyjaszewski, K. *Eur. Phys. J. E: Soft Matter* **2003**, *10*, 5.
(89) Ejaz, M.; Yamamoto, S.; Ohno, K.; Tsujii, Y.; Fukuda, T. *Macromolecules* **1998**, *31*, 5934.
(90) Matyjaszewski, K.; Miller, P. J.; Shukla, N.; Immaraporn, B.; Gelman, A.; Luokala, B. B.; Siclovan, T. M.; Kickelbick, G.; Vallant, T.; Hoffmann, H.; Pakula, T. *Macromolecules* **1999**, *32*, 8716.
(91) Zhao, B.; Brittain, W. J. *Prog. Polym. Sci.* **2000**, *25*, 677.
(92) Pyun, J.; Matyjaszewski, K. *Chem. Mater.* **2001**, *13*, 3436.
(93) Pyun, J.; Kowalewski, T.; Matyjaszewski, K. *Macromol. Rapid Commun.* **2003**, *24*, 1043.
(94) Luzinov, I.; Minko, S.; Tsukruk, V. V. *Prog. Polym. Sci.* **2004**, *29*, 635.
(95) Miller, P. J.; Matyjaszewski, K. *Macromolecules* **1999**, *32*, 8760.
(96) Keller, R. N.; Wycoff, H. D. *Inorg. Synth.* **1946**, *2*, 1.
(97) Zhao, D.; Feng, J.; Huo, Q.; Melosh, N.; Frederickson, G. H.; Chmelka, B. F.; Stucky, G. D. *Science* **1998**, *279*, 548.
(98) Matos, J. R.; Kruk, M.; Mercuri, L. P.; Jaroniec, M.; Zhao, L.; Kamiyama, T.; Terasaki, O.; Pinnavaia, T. J.; Liu, Y. *J. Am. Chem. Soc.* **2003**, *125*, 821.
(99) Yu, C.; Yu, Y.; Zhao, D. *Chem. Commun.* **2000**, 575.
(100) Matyjaszewski, K.; Jo, S. M.; Paik, H.-j.; Gaynor, S. G. *Macromolecules* **1997**, *30*, 6398.
(101) Matyjaszewski, K.; Jo, S. M.; Paik, H.-j.; Shipp, D. A. *Macromolecules* **1999**, *32*, 6431.
(102) Tang, C.; Kowalewski, T.; Matyjaszewski, K. *Macromolecules* **2003**, *36*, 1465.
(103) Sing, K. S. W.; Everett, D. H.; Haul, R. A. W.; Moscou, L.; Pierotti, R. A.; Rouquerol, J.; Siemieniewska, T. *Pure Appl. Chem.* **1985**, *57*, 603.
(104) Kruk, M.; Jaroniec, M.; Bereznitski, Y. *J. Colloid Interface Sci.* **1996**, *182*, 282.
(105) Barrett, E. P.; Joyner, L. G.; Halenda, P. P. *J. Am. Chem. Soc.* **1951**, *73*, 373.
(106) Kruk, M.; Jaroniec, M.; Sayari, A. *Langmuir* **1997**, *13*, 6267.
(107) Jaroniec, M.; Kruk, M.; Olivier, J. P. *Langmuir* **1999**, *15*, 5410.
(108) Ryoo, R.; Ko, C. H.; Kruk, M.; Antochshuk, V.; Jaroniec, M. *J. Phys. Chem. B* **2000**, *104*, 11465.
(109) Kruk, M.; Celer, E. B.; Jaroniec, M. *Chem. Mater.* **2004**, *16*, 698.
(110) Kruk, M.; Jaroniec, M.; Ryoo, R.; Joo, S. H. *J. Phys. Chem. B* **2000**, *104*, 7960.
(111) Kruk, M.; Jaroniec, M.; Kim, T.-W.; Ryoo, R. *Chem. Mater.* **2003**, *15*, 2815.
(112) Shin, H. J.; Ryoo, R.; Kruk, M.; Jaroniec, M. *Chem. Commun.* **2001**, 349.
(113) Yoon, S. B.; Kim, J. Y.; Kooli, F.; Lee, C. W.; Yu, J.-S. *Chem. Commun.* **2003**, 1740.
(114) Fan, J.; Yu, C.; Wang, L.; Tu, B.; Zhao, D.; Sakamoto, Y.; Terasaki, O. *J. Am. Chem. Soc.* **2001**, *123*, 12113.
(115) Sonobe, N.; Kyotani, T.; Hishiyama, Y.; Shiraishi, M.; Tomita, A. *J. Phys. Chem.* **1988**, *92*, 7029.